Trends in Na-Ion Solvation with Alkyl-Carbonate Electrolytes for Sodium-Ion Batteries: Insights from First-Principles Calculations

ARTICLE *in* THE JOURNAL OF PHYSICAL CHEMISTRY C · JULY 2015

Impact Factor: 4.77 · DOI: 10.1021/acs.jpcc.5b04706

5 AUTHORS, INCLUDING:

Mehdi Shakorian
Birjand University of Technology
30 PUBLICATIONS **94** CITATIONS
SEE PROFILE

Ganesh Kamath
50 PUBLICATIONS **577** CITATIONS
SEE PROFILE

Hui Xiong
Boise State University
22 PUBLICATIONS **873** CITATIONS
SEE PROFILE

Subramanian K. R. S. Sankaranarayanan
Argonne National Laboratory
106 PUBLICATIONS **639** CITATIONS
SEE PROFILE

THE JOURNAL OF PHYSICAL CHEMISTRY C

Article

pubs.acs.org/JPCC

Trends in Na-Ion Solvation with Alkyl-Carbonate Electrolytes for Sodium-Ion Batteries: Insights from First-Principles Calculations

Mehdi Shakourian-Fard,[†] Ganesh Kamath,[*,†] Kassiopeia Smith,[‡] Hui Xiong,[‡] and Subramanian K. R. S. Sankaranarayanan[*,§]

[†]Department of Chemistry, University of Missouri−Columbia, Columbia, Missouri 65211, United States

[‡]Department of Material Science and Engineering, Boise State University, 1910 University Drive, Boise, Idaho 83725, United States

[§]Center for Nanoscale Materials, Argonne National Laboratory, 9700 South Cass Avenue, Argonne, Illinois 60439, United States

Supporting Information

ABSTRACT: Classical molecular dynamics (MD) simulations and M06-2X hybrid density functional theory calculations have been performed to investigate the interaction of various nonaqueous organic electrolytes with Na^+ ion in rechargeable Na-ion batteries. We evaluate trends in solvation behavior of seven common electrolytes namely pure carbonate solvents (ethylene carbonate (EC), vinylene carbonate (VC), propylene carbonate (PC), butylene carbonate (BC), dimethyl carbonate (DMC), ethyl methyl carbonate (EMC), and diethyl carbonate (DEC)) and four binary mixtures of carbonates (EC:PC, EC:DMC, EC:EMC, and EC:DEC). Thermochemistry calculations for the interaction of pure and binary mixtures of carbonate solvents with Na^+ ion, Na^+ ion coordinated with carbonate clusters obtained from molecular dynamics simulations, show that the formation of Na-carbonate complexes is exothermic and proceeds favorably. Based on the highest binding energy (ΔE_b), enthalpy of solvation ($\Delta H_{(sol)}$), and Gibbs free energy of solvation ($\Delta G_{(sol)}$) values for the interaction of Na^+ ion with carbonate solvents, our results conclusively show that pure EC and binary mixture of (EC:PC) are the best electrolytes for sodium-ion based batteries. Quantum chemical analyses are performed to understand the observed trends in ion solvation. Quantum theory of atoms in molecules (QTAIM) analysis shows that the interactions in Na-carbonate complexes are classified as a closed-shell (electrostatic) interaction. The localized molecular orbital energy decomposition analysis (LMO-EDA) also indicates that the electrostatic term (ΔE_{ele}) in the interaction energy between Na^+ ion and carbonate solvents has the highest value and confirms the results of QTAIM about the electrostatic nature of Na^+ ion interaction. The noncovalent interaction (NCI) plots indicate that the noncovalent interactions responsible for the formation of Na-carbonate complexes are strong to weak attractive interactions. Density of state (DOS) calculations show that the HOMO−LUMO energy gap in the EC, VC, PC, BC, DMC, EMC, and DEC increases as they interact with Na^+ ion, although the HOMO−LUMO energy gap decreases with the addition of EC as an electrolyte additive to PC, DMC, and EMC. Calculated trends based on these quantum chemical calculations suggest that EC and binary mixture of EC:PC emerge as the best electrolytes in sodium-ion batteries, which is in excellent agreement with previously reported in silico experimental results.

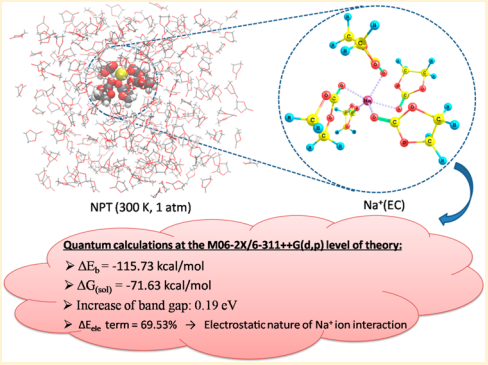

1. INTRODUCTION

With an ever growing need for energy, a considerable amount of effort is being focused on reducing the anthropogenic carbon footprint, and with a number of candidate renewable sources making a way into the energy market, energy storage technology such as rechargeable battery has attempted to establish a niche in the portable electronic industry and high performance electric vehicles.[1−3] However, battery technology which is primarily driven by lithium-ion based technology faces real challenges in terms of availability and cost. It is estimated that with the present demand for lithium, the resources based on raw lithium material, that is, lithium carbonates, would last for a century or less.[4−7] In anticipation of such a scenario, alternative technologies beyond lithium need to be developed.[8−12] Ever since the successful development of high temperature Na/S||Na/$NiCl_2$ Zebra sodium with Na^+-β-alumina ceramic electrolyte in 1985, sodium-ion based technology has been a torch bearer for "beyond lithium" technologies.[13] Although the theoretical energy density of Na^+ ions is lower than Li^+ ion due to its higher weight, various salient features, including abundant availability and low cost per ton, make this avenue worthy of exploration. It is worth mentioning that the efficiency of the Na-ion battery (NIB) is comparable with Li-ion battery (LIB). If a rechargeable NIB with good performance characteristics could be developed, it could have the advantage of using electrolyte systems with

Received: May 17, 2015
Revised: August 20, 2015
Published: September 15, 2015

DOI: 10.1021/acs.jpcc.5b04706
J. Phys. Chem. C 2015, 119, 22747−22759

Scheme 1. Chemical Structure of Various Nonaqueous Organic Electrolytes Whose Interactions with Sodium Ion are Studied in This Work

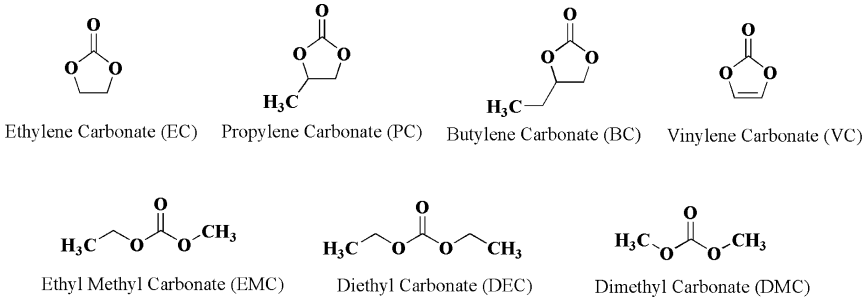

lower decomposition potential due to the higher half-reaction potential for sodium relative to lithium. In addition, given the lower operating voltage of NIB, it would provide enhanced stability to nonaqueous battery electrolytes as compared to Li-ion batteries.

In order to compete and go beyond the existing Li-ion technology, a significant advancement in our understanding of electrodes, electrolytes, and interfacial dynamics is needed. The scientific community has been actively focused on electrode materials for lithium-ion batteries[14−17] and studies based on optimal selection of electrolytes for Na-ion batteries under scrutiny.[18−20] Furthermore, a large number of experimental,[21−23] quantum chemical,[24−27] and molecular dynamics simulation[26,28,29] studies have been performed to understand how Li^+ ion interacts with organic solvent molecules, mostly carbonates with different ether and carbonyl oxygen containing species and their mixtures. It is worth mentioning that the electrolytes that perform well for Li-ion batteries do not guarantee their suitability for Na-ion batteries, although they may share similar chemistries. For example, EC:DMC or EC:DEC has been found to be the most stable electrolyte mixture in Li-ion batteries, although the results of molecular dynamics simulation have recently shown that EC:PC can be the most suitable electrolyte mixture for Na-ion batteries.[7] Hence, a systematic investigation for the choice of optimal electrolytes for Na-ion batteries is needed. Additionally, the selection and optimization of binders, additives, and electrolyte all have a significant impact on the electrochemical behavior of negative electrodes, which dictates with formation of surface passivation layers, namely, solid electrolyte interphase (SEI). For example, the degradation reactions of nonaqueous electrolytes often take place near the graphite anode materials in Na-ion batteries, which result in insoluble products adhering to the negative electrode surface and forming the protective solid passivation layer, SEI.[21]

Although not comprehensive, there has been a recent molecular dynamics simulation that has attempted to optimize the electrolyte formulations for Na^+-ion batteries.[7] On the other hand, Okoshia et al.[30] in a study theoretically evaluated the desolvation energies of Li, Na, and Mg ions to 27 organic electrolyte solvents. They showed that the Na-ion complexes revealed commonly smaller desolvation energies compared to the Li-ion complexes due to the weaker Lewis acidity, while the solvation structures were similar to each other. The Mg-ion complexes showed remarkably larger desolvation energies because of the double positive charge.

In order to achieve optimal electrolytes for Na-ion batteries, recently our group performed an integrated computational (molecular dynamics simulations)−experimental approach and rank-ordered various nonaqueous electrolytes for a Na-ion battery based on thermodynamic and kinetic properties.[7] We have established in our prior work that if the electrolyte is compatible with the constitute ion, it would result in efficient transport of the ions across the electrodes. Hence, we used solvation-free energy and kinetic factors as metrics for evaluating the rank order of the cyclic and acyclic carbonates with Na^+ ion. Despite this recent study, a fundamental understanding of the Na^+ ion solvation behavior at the electronic structure level is still lacking.

In this work, we perform detailed electronic structure calculations to further understand the evolving picture of ion-electrolyte compatibility. We seek to identify additional descriptors based on the electronic and quantum level interactions that would complement our previous integrated molecular dynamics-experimental approach, enabling effective screening protocols of electrolyte optimization and aiding in rational design. We limit our focus to understanding trends in solvation behavior of Na^+ ions with carbonates (the optimal clusters obtained from molecular dynamics simulations of sodium ion with various carbonates) and the associated charge distribution flow based on nonreactive model chemistries. Of particular interest is determining the quantum mechanical properties such as relative HOMO−LUMO energy band gap, amount and direction of charge transfer, and charge redistribution upon interaction of the sodium ion with the various electrolytes. A further insight would be to understand the relationship of such quantities to the binding energetics of the ion with the electrolytes and solvation dynamics and structural behavior of electrolytes with the ion. Further, it is our understanding that such properties would have a bearing on the charging−discharging mechanism of nonaqueous liquid electrolytes. Toward this goal, in this present study, we use quantum chemical calculations to systematically investigate the solvation of sodium ion in various nonaqueous electrolytes (cyclic and acyclic carbonates) and their combinations (Scheme 1).

2. COMPUTATIONAL DETAILS

2.1. Generation of Initial Configurations. There are several advanced sampling strategies that are available such as the evolutionary approaches such as Genetic Algorithms,[31] Neural Networks,[32] and DFT-based clustering,[26,28,29,33−36] to name a few. Here, we sample the initial configurations used for electronic structure calculations from an extensive molecular dynamics (MD) simulation trajectory. MD simulations were performed with NAMD, version 2.9.[37] Initial configurations for each system were generated with Packmol software. Energy minimization was performed on all systems for 500 steps using the steepest decent technique. Systems were equilibrated over a

DOI: 10.1021/acs.jpcc.5b04706
J. Phys. Chem. C 2015, 119, 22747−22759

time period of 20.0 ns in isobaric−isothermal ensemble at 1.0 atm and 300 K. The number of carbonates was selected based on the density in a 30 × 30 × 30 Å^3. Further molecular dynamics simulation details could be found in our earlier article.[7]

From these trajectories for the various sodium ion-carbonate systems, we had stored 20000 configurations. Based on a distance criteria of Na^+-O (oxygen of the carbonate) distance of 3.0 Å, we calculated a variety of Na-coordinated clusters. Figure S1 provides the distribution of such various size Na-coordinated carbonate clusters for the seven neat carbonates. Table S1 provides the distribution of the various clusters in the binary alkyl carbonate systems. The maximum probable cluster size for each carbonate system was determined. These resulted in cluster configurations >10000. These clusters were used as input structures and single point energies of these clusters were determined at M06-2X/6-311++G(d,p) level of theory. The minimum energy of these clusters was taken as the ground state and the relative QM single point energies were computed. Further, these cluster energies were also determined using CHARMM general force field (CGENFF).[38] For all the systems, the lowest energy based on QM and force field was for the same cluster configuration. A perfect ordering of the cluster configuration for the minimum energy configurations is seen as determined by QM and force field.

2.2. Cross-Validation of the Force Field and Configurational Sampling. Figure 1 shows the comparison between the relative configurational energies derived from our force field with those obtained from quantum calculations at the M06-2X/6-311++G(d,p) level of theory and basis set. Note the extensively large of configurations sampled (>10000 for each of the different electrolyte systems) from the MD trajectories. By employing such a large cross-validation test set, we ensure that the test set represents structures with diverse local solvation coordination and amply samples the energy landscape. We find that there is an excellent correlation between the predictions of the force fields and the quantum calculations; the correlation coefficient being ∼0.9 for most cases. The mean absolute error (average of the absolute errors), which is a measure of how close the predictions of force fields are to the eventual outcomes computed by quantum calculations, is within 0.5 kcal/mol for all the cases, which suggests an excellent agreement. Also, a comparison of the energetic ordering of the solvated structures between the force field and the quantum calculations shows excellent agreement. Given the remarkable accuracy of the force field employed in this work, it is reasonable to expect that the lowest energy configuration clusters chosen from a diverse set of MD configurations adequately represent the most thermodynamically stable cluster structures upon which further quantum calculations can be performed. The analysis presented in this paper,[33] where the authors have identified to most stable cluster structures is indeed an elegant technique and represents a powerful alternative technique if reliable force fields are unavailable. Given the accuracy of recent force fields, one of the main aims of this paper is to illustrate how one can sample configurations using molecular dynamics and perform detailed electronic structure calculations on the same to gain useful insights into an important class of electrolyte systems.

2.3. Electronic Structure Calculations. The Gaussian 09 package[39] was employed for all ab initio calculations and density functional calculations using the M06-2X functional developed by Truhlar et al.[40] The basis set was chosen as 6-311++G(d,p) for our calculations. The geometry optimization of various nonaqueous electrolytes (cyclic and acyclic carbonates) as well as their complexes with Na^+ ion was carried out without symmetry restrictions in the singlet ground state. The absence of imaginary frequencies in the calculated

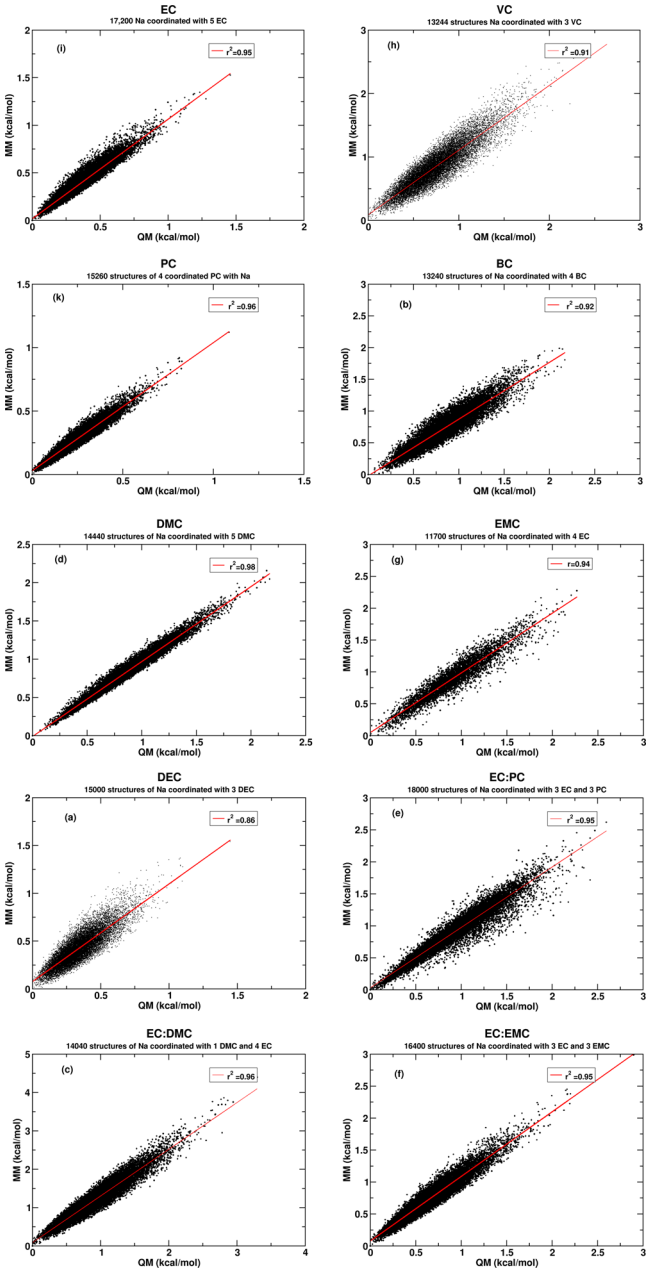

Figure 1. Comparison of force field (FF) derived configurational energies (relative to lowest energy configuration) vs those calculated at M06-2X/6-311++G(d,p) level of theory and basis set for an extensively large number of solvated structures sampled from long time scale molecular dynamics trajectories. Each of the different panels shows the comparison for a given electrolyte. We note that there is an excellent correlation between the energies predicted by CGENFF with respect to quantum calculations. Most importantly, the mean absolute error (MEA) is less than 0.5 kcal/mol, which suggests that the energetic description of the solvated clusters by the FF employed is quite accurate. Additionally, we also find that the energetic ordering predicted by our FF matches very well with the quantum calculations. The correlation coefficient r^2 is determined for the sodium ion-carbonate systems.

DOI: 10.1021/acs.jpcc.5b04706
J. Phys. Chem. C 2015, 119, 22747−22759

vibrational frequencies of the optimized structures ensured that structures are stable. Zero-point energy (ZPE) corrections were calculated and taken into account for the calculation of binding energy (ΔE_b). For all the complexes, binding energy values were calculated based on the difference in energy between the complex and the constituents of the complex (carbonate molecule (CM) and Na^+ ion; $\Delta E_b = E_{(complex)} - (n \cdot E_{(CM)} + E_{(Na^+ ion)})$. The basis set superposition errors (BSSE) were calculated using Boys–Bernardi's counterpoise procedure (CP) and added to the binding energies.[41]

In addition to binding energy, enthalpy, and free energy of solvation ($\Delta H_{(sol)}$ and $\Delta G_{(sol)}$, respectively) of Na^+ ion with the carbonate molecules at 298.15 K were calculated using eq 1:

$$\Delta X_{(sol)} = X_{(complex)} - (n \cdot X_{(CM)} + X_{(Na^+ ion)}) \quad (1)$$

where X = H and G. The entropy (S) of solvation was also calculated at 298.15 K from eq 2.

$$\Delta S_{(sol)} = \frac{(\Delta H_{(sol)} - \Delta G_{(sol)})}{298.15} \quad (2)$$

Within the NBO analysis introduced by Weinhold and co-workers,[42] we paid particular attention to natural population analysis (NPA) charges[43] and charge transfers. Density of states of carbonate solvents and all complexes, including the Na^+ ion, were also calculated. To reveal the binding strength of the Na^+ ion with carbonate solvents and their mixtures, the quantum theory of atoms in molecules (QTAIM)[44] analysis was carried out on all optimized complexes. The localized molecular orbital energy decomposition analysis (LMO-EDA), which was developed by Su et al.[45] was done using the GAMESS software[46,47] to determine the contributions of interaction energy terms. The bonding analysis was carried out at the M06-2X/6-311++G(d,p) level of theory. Finally, the visualization of noncovalent interaction regions was conducted using the Multiwfn-3.2 program,[48] and then the graphics for the noncovalent interactions were rendered using the VMD 1.9.2 software.[49]

3. RESULTS AND DISCUSSION

3.1. Geometries and Relative Stabilities. The initial structures for investigation of the interaction of Na^+ ion with nonaqueous solvents of EC, VC, PC, BC, DMC, EMC, DEC, and the mixtures of EC:PC, EC:DMC, EC:EMC, and EC:DEC were taken from performed molecular dynamics simulations and then optimized at the M06-2X/6-311++G(d,p) level of theory. The optimized structures of these complexes are shown in Figure 2. As shown in Figure 2, the favorable site for interaction of Na^+ ion with nonaqueous solvents is near the carbonyl oxygen atom. Especially for the regions around the ethereal oxygen atoms, there are no signs indicating the possibility of strong interactions with ions. These results are consistent with the MD simulation results reported recently by Kamath et al.[7]

The basic solvation geometry around the Na^+ ion among the various complexes is different in the primary solvation sphere (Figure 2). In some cases, one or two cyclic and acyclic carbonates move out the primary solvation sphere and form the second solvation sphere. These carbonate molecules in the second solvation sphere are weakly bonded to other carbonate molecules in the primary solvation sphere by interactions between oxygen atoms and hydrogen atoms of $-CH_3$, $-CH_2$, and $-CH$ groups in the carbonate molecules.

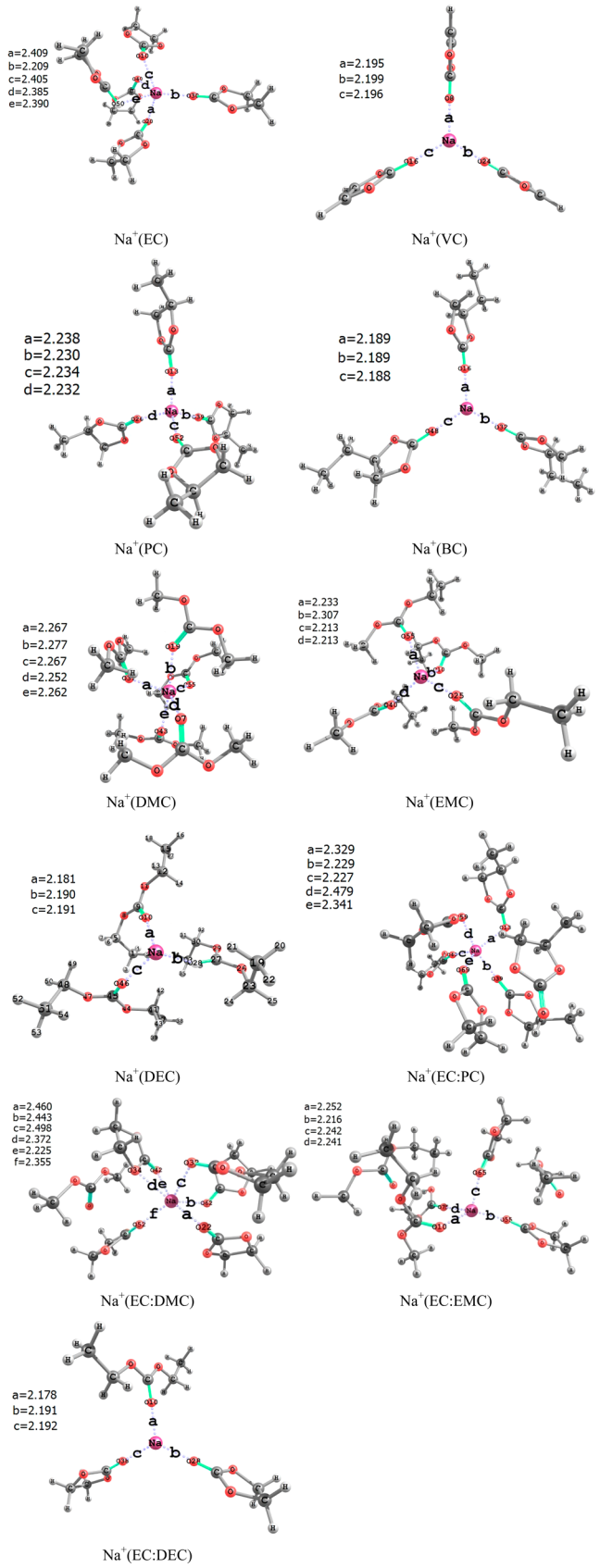

Figure 2. Optimized structures for the interaction of Na^+ ion with nonaqueous carbonates: EC, VC, PC, BC, DMC, EMC, and DEC, and the mixtures of EC:PC, EC:DMC, EC:EMC, and EC:DEC.

DOI: 10.1021/acs.jpcc.5b04706
J. Phys. Chem. C 2015, 119, 22747–22759

Table 1. Average $Na^+\cdots O$ Bond Lengths (in Å), Dielectric Constant (ε)[7] of Carbonate Solvents, Binding Energy (ΔE_b in kcal/mol) Corrected by Basis Set Super Position Error (BSSE), Enthalpy of Solvation ($\Delta H_{(sol)}$ in kcal/mol), Free Energy of Solvation ($\Delta G_{(sol)}$ in kcal/mol), and Entropy of Solvation ($\Delta S_{(sol)}$ in cal/mol·K) of Na^+ Ion by Carbonate Molecules

structure	ΔE_b	$\Delta H_{(sol)}$	$\Delta G_{(sol)}$	$\Delta S_{(sol)}$	ε	$r_{Na^+\cdots O}$
Na^+(EC)	−115.73	−122.05	−71.63	−169.12	89.78	2.359
Na^+(VC)	−79.22	−79.70	−56.60	−77.45	126	2.196
Na^+(PC)	−101.16	−101.79	−69.36	−108.80	64.92	2.233
Na^+(BC)	−88.08	−88.50	−64.13	−81.73	56.10	2.189
Na^+(DMC)	−97.71	−105.31	−45.59	−200.31	3.11	2.265
Na^+(EMC)	−88.68	−92.84	−50.37	−142.46	2.96	2.241
Na^+(DEC)	−74.08	−77.02	−46.07	−103.79	2.81	2.187
Na^+(EC:PC)	−132.41	−141.41	−77.25	−215.21		2.321
Na^+(EC:DMC)	−127.40	−137.54	−70.72	−224.14		2.392
Na^+(EC:EMC)	−123.98	−133.35	−66.05	−225.73		2.238
Na^+(EC:DEC)	−82.78	−83.40	−60.11	−78.13		2.187

The average $Na^+\cdots O$ bond lengths in the primary solvation sphere in these complexes are summarized in Table 1. The $Na^+\cdots O$ bond lengths in these complexes depend on the type, arrangement, and number of carbonate solvents around Na^+ ion. The average $Na^+\cdots O$ bond lengths in Na^+(EC), Na^+(VC), Na^+(PC), Na^+(BC), Na^+(DMC), Na^+(EMC), and Na^+(DEC) complexes are 2.359, 2.196, 2.233, 2.189, 2.265, 2.241, 2.187 Å, respectively.

Comparison of Na^+(EC), Na^+(PC), and Na^+(BC) complexes suggests that the number of EC, PC, and BC molecules in the primary solvation sphere around the Na^+ ion decreases with the increase of the size of solvents from EC to BC. In addition, the average $Na^+\cdots O$ bond length in these complexes decreases from 2.359 Å in Na^+(EC) to 2.189 Å in Na^+(BC) complex due to the decrease of steric hindrance between carbonate solvents and thus their more flexibility in the primary solvation sphere. A similar result is seen in Na^+(DMC), Na^+(EMC), and Na^+(DEC) complexes. As seen in Figure 2, the number of DMC, EMC, and DEC molecules in the Na^+(DMC), Na^+(EMC), and Na^+(DEC) complexes decreases with the increase of the size of carbonate solvents from DMC to DEC, respectively. In agreement with the decrease in the number of carbonate solvents in the primary solvation sphere, the steric hindrances between carbonate solvents decreases, and thus the average $Na^+\cdots O$ bond length decreases.

With the addition of EC as an electrolyte additive to PC, DMC, EMC, and DEC carbonate solvents, some changes are observed in the average $Na^+\cdots O$ bond lengths, geometries, and the number of carbonate solvents around Na^+ ion. When EC is added to PC electrolyte, two PC and three EC solvents stay in the primary solvation sphere and the average $Na^+\cdots O$ bond length increases from 2.233 to 2.321 Å. Generally, with the addition of EC electrolyte to DMC, EMC, and DEC solvents the EC molecules indicate a stronger interaction with Na^+ ion in the primary solvation sphere than DMC, EMC, and DEC solvents, and thus, a higher number of EC molecules stay in the primary solvation sphere. In addition, the average $Na^+\cdots O$ bond length in these complexes decreases from 2.392 Å in Na^+(EC:DMC) complex to 2.187 Å in Na^+(EC:DEC) complex. Thus, the magnitude of sodium ion interaction with the oxygen (electronegative atom) of the carbonate is an indication of cluster formation and also shows the compatibility of the ion with the various carbonates. It is indicative of measure of solvating nature of the carbonates for the particular ion and serves as a descriptor for thermodynamic considerations of cluster formation.

The binding energy (ΔE_b), enthalpy of solvation ($\Delta H_{(sol)}$), free energy of solvation ($\Delta G_{(sol)}$), and entropy of solvation ($\Delta S_{(sol)}$) of Na^+ ion by carbonate molecules are summarized in Table 1. The binding energy value between Na^+ ion and carbonate solvents is controlled by the types of intermolecular interactions. These interactions are further identified in Localized Molecular Orbital Energy Decomposition Analysis (LMO-EDA) and also shown by noncovalent interaction (NCI) plots. Based on the binding energy values in Table 1, it is obvious that the binding energy is strongly dependent on the type and number of carbonate molecules coordinated to Na^+ ion and the coordination mode of Na^+ ion to the carbonate molecules.[50,51] A comparison between the binding energy (ΔE_b) values for Na-acyclic, Na-cyclic, and Na-binary mixture complexes are shown in Figure 3. As seen from Figure 3, the

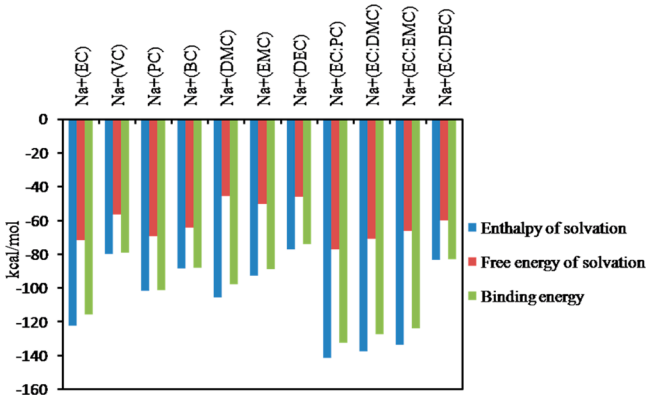

Figure 3. Comparison of binding energy (ΔE_b), enthalpy of solvation ($\Delta H_{(sol)}$), and free energy of solvation ($\Delta G_{(sol)}$) of Na^+ ion by EC, VC, PC, BC, DMC, EMC, and DEC and the mixtures of EC:PC, EC:DMC, EC:EMC, and EC:DEC.

highest binding energy for the interaction of Na^+ ion with the carbonate molecules in the complexes containing only one type of carbonate molecules is seen for the Na^+(EC) (−115.73 kcal/mol) complex. On the other hand, when the Na^+ ion is solvated by the binary mixtures of carbonate molecules, the highest binding energy value is seen for the Na^+(EC:PC) (−132.41 kcal/mol) complex (Figure 3).

The rank order for the magnitude of binding energy between Na^+ ion and pure carbonate molecules as well as their binary mixtures ranging from maximum to minimum affinity is as follows: Na^+(EC:PC) (−132.41 kcal/mol) > Na^+(EC:DMC)

DOI: 10.1021/acs.jpcc.5b04706
J. Phys. Chem. C 2015, 119, 22747−22759

(−127.40 kcal/mol) > Na^+(EC:EMC) (−123.98 kcal/mol) > Na^+(EC) (−115.73 kcal/mol) > Na^+(PC) (−101.16 kcal/mol) > Na^+(DMC) (−97.71 kcal/mol) > Na^+(EMC) (−88.68 kcal/mol) > Na^+(BC) (−88.08 kcal/mol) > Na^+(EC:DEC) (−82.78 kcal/mol) > Na^+(VC) (−79.22 kcal/mol) > Na^+(DEC) (−74.08 kcal/mol), respectively. It is worth mentioning that the maximum affinity of Na^+ ion is seen with ethylene carbonate (EC) and the combination of ethylene carbonate with propylene carbonate (EC:PC) having the highest order for this descriptor complies with our previous MD simulations.[7]

3.2. Thermochemistry of Na^+ Ion Solvation by Carbonate Solvents. In designing new electrolytes, it is generally desired that the solubility of the salt in nonaqueous solvents are high. Our basic hypothesis is that for a successful ion−solvent system the ion should have a favorable free energy of solvation in a particular solvent. As a rank-order criterion, we calculated the enthalpy of solvation ($\Delta H_{(sol)}$), Gibbs free energy of solvation ($\Delta G_{(sol)}$), and entropy of solvation ($\Delta S_{(sol)}$) for different Na-carbonate combinations and ranked them based on the magnitude of Gibbs free energies of solvation.

The enthalpy of solvation ($\Delta H_{(sol)}$) for the complexes of carbonate solvents with Na^+ ion is presented in Table 1. The $\Delta H_{(sol)}$ values for these complexes are negative (exothermic reactions), suggesting that the formation of Na-carbonate complexes is favorable. The rank order for the magnitude of $\Delta H_{(sol)}$ for the complexes of isolated carbonate molecules and their mixtures with Na^+ ion is as follows: Na^+(EC:PC) (−141.41 kcal/mol) > Na^+(EC:DMC) (−137.54 kcal/mol) > Na^+(EC:EMC) (−133.35 kcal/mol) > Na^+(EC) (−122.05 kcal/mol) > Na^+(DMC) (−105.31 kcal/mol) > Na^+(PC) (−101.79 kcal/mol) > Na^+(EMC) (−92.84 kcal/mol) > Na^+(BC) (−88.50 kcal/mol) > Na^+(EC:DEC) (−83.40 kcal/mol) > Na^+(VC) (−79.70 kcal/mol) > Na^+(DEC) (−77.02 kcal/mol), respectively. As seen from Figure 3, the highest $\Delta H_{(sol)}$ value for the interaction of Na^+ ion with carbonate solvents in the complexes containing only one type of carbonate molecules is seen for Na^+(EC) complex. On the other hand, the highest $\Delta H_{(sol)}$ value for the interaction of Na^+ ion with combination of carbonates is seen for Na^+(EC:PC) complex.

The Gibbs free energy of solvation ($\Delta G_{(sol)}$) is defined as the difference in Gibbs free energy between the complex and the constituents of the complex [carbonate solvents and Na^+ ion; $\Delta G_{(sol)} = G_{(complex)} - (G_{(CM)} + G_{(Na^+ion)})$]. The differences in the free energies of Na^+ ion in the seven pure carbonate solvents and four binary mixtures of carbonates are presented in Figure 3. The $\Delta G_{(sol)}$ values for these complexes are negative. Therefore, it is expected that the solvation of Na^+ ion proceeds favorably in all the above complexes. The rank order for the magnitude of $\Delta G_{(sol)}$ for the complexes is as follows: Na^+(EC:PC) (−77.25 kcal/mol) > Na^+(EC) (−71.63 kcal/mol) > Na^+(EC:DMC) (−70.72 kcal/mol) > Na^+(PC) (−69.36 kcal/mol) > Na^+(EC:EMC) (−66.05 kcal/mol) > Na^+(BC) (−64.13 kcal/mol) > Na^+(EC:DEC) (−60.11 kcal/mol) > Na^+(VC) (−56.60 kcal/mol) > Na^+(EMC) (−50.37 kcal/mol) > Na^+(DEC) (−46.07 kcal/mol) > Na^+(DMC) (−45.59 kcal/mol), respectively.

As seen from Figure 3, the highest $\Delta G_{(sol)}$ value for the interaction of Na^+ ion with pure carbonate solvents is seen for Na^+(EC) (−71.63 kcal/mol) complex, indicating EC as a better solvent in comparison with VC, PC, BC, DMC, EMC, and DEC in applications of sodium ion batteries. On the other hand, the highest $\Delta G_{(sol)}$ value for the interaction of Na^+ ion with four binary mixtures of carbonates (EC:PC, EC:DMC, EC:EMC, and EC:DEC) is seen for Na^+(EC:PC) (−77.25 kcal/mol) complex, indicating EC:PC as a better binary solvent among other binary mixtures of carbonates in applications of sodium ion batteries. It is interesting to note that the choice of EC and EC:PC based on having the highest Gibbs free energy solvation as the best solvents for application in sodium ion batteries is in good agreement with our results from molecular dynamics simulations.[7] On the other hand, based on the $\Delta G_{(sol)}$ values in Figure 3, the worst acyclic, cyclic, and binary mixture solvents for application in sodium ion batteries are Na^+(DMC), Na^+(VC), and Na^+(EC:DEC), respectively.

The Gibbs free energy of solvation ($\Delta G_{(sol)}$) from our computation is plotted against the literature compiled dielectric constant of carbonate solvents, see Figure 4. Note that Zhou et al.[52] have shown the dependence of electrostatic solvation energy of a charged species on dielectric constant of solvent. Based on our solvation model, we observe that the magnitude of the electrostatic solvation energy decreases with decreasing static dielectric constant of the solvent. As seen from Figure 4, the free energy of solvation of Na^+ ion in acyclic carbonates is less than cyclic carbonates. On the other hand, the $\Delta G_{(sol)}$ values decrease with the increase of the number of carbon atoms in acyclic and cyclic carbonates. Clearly one sees that VC is an outlier for this correlation and the aromatic with the double bond characteristics of VC could be attributed to the observed anomaly of increased dielectric constant.

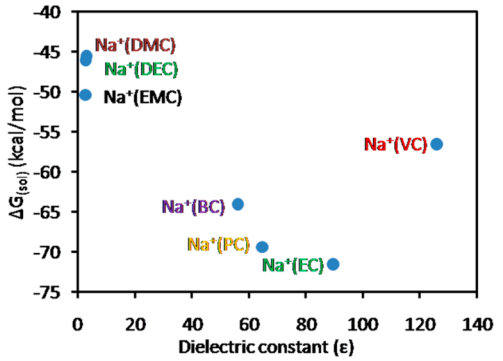

Figure 4. Comparison of the free energy of solvation of Na^+ ion in various acyclic/cyclic carbonates.

Finally, the entropy of solvation ($\Delta S_{(sol)}$) was calculated by eq 2. The negative values of entropy in Table 1 indicate that the entropy decreases upon interaction of carbonate solvents with Na^+ ion, which is due to the decreased translation degree of freedom of the carbonate molecules.

A key aspect of good electrolyte for metal-ion batteries is their relative ability to solvate and desolvate the ion. Based on the magnitude of the thermochemistry values, at the level of M06 model chemistry, it would suggest that the ion−solvent complexing is exothermic and spontaneous. However, one can argue that, if the ion solvating nature of the solvent is large, desolvation would require an energy penalty. We would like to note that this desolvation or reverse process can be made favorable by increasing the temperature of the system. The efficiency of the battery would then be dependent on the relative energy demands of solvation/desolvation. Alternatives would include the use of additives and design of electrodes, which have a larger free energy of interaction with the ion, thereby aiding in the desolvation process. We further note that

DOI: 10.1021/acs.jpcc.5b04706
J. Phys. Chem. C 2015, 119, 22747−22759

these calculations are to determine the compatibility of ions with various solvents emulating the bulk behavior.

3.3. Natural Bond Orbital (NBO) and Quantum Theory of Atoms in Molecules (QTAIM) Analyses. To gain further insights into the extent of charge transfer in these complexes, natural population analysis (NPA) was calculated by the NBO method at the M06-2X/6-311++G(d,p) level of theory. Charge distribution of the metal ion, charge transfer, the sum of perturbative stabilization energies ($\sum\Delta E_{CT}$), the sum of Na^+−O Wiberg bond index[53] ($\sum b_{Na^+-O}$), and the sum of electron density ($\sum\rho(r)$) at the BCPs of Na^+−O bonds for the interaction of carbonate molecules with Na^+ ion are summarized in Table 2. In all complexes, the charge transfer

Table 2. Natural Population Analysis (NPA) Charges on Na^+ Ion in the Complexes (q_{Na^+} in |e|), Charge Transfer ($\Delta q_{Na^+} = q_{Na^+(isolated)} - q_{Na^+(complexed)}$), the Sum of Perturbative Stabilization Energies ($\sum\Delta E_{CT}$; in kcal/mol) for Na^+−O Bonds, the Sum of Na^+−O Wiberg Bond Index ($\sum b_{Na^+-O}$), and the Sum of Electron Density ($\sum\rho(r)$ Resulted from Atoms in Molecules Analysis) in the Bond Critical Points of Na^+−O Bonds in the Primary Solvation Sphere

structure	q_{Na^+}	Δq_{Na^+}	$\sum\Delta E_{CT}$	$\sum\rho(r)$	$\sum b_{Na^+-O}$
Na^+(EC)	0.73846	0.26154	115.05	0.0882	0.348
Na^+(VC)	0.91493	0.08507	46.64	0.0722	0.153
Na^+(PC)	0.84715	0.15285	78.39	0.0838	0.268
Na^+(BC)	0.91045	0.0895	45.03	0.0741	0.1602
Na^+(DMC)	0.58880	0.4112	154.60	0.1085	0.411
Na^+(EMC)	0.77352	0.22648	78.04	0.0913	0.250
Na^+(DEC)	0.87405	0.12595	31.94	0.0772	0.118
Na^+(EC:PC)	0.75150	0.2485	116.68	0.0939	0.3619
Na^+(EC:DMC)	0.71190	0.2881	137.95	0.0986	0.4123
Na^+(EC:EMC)	0.80981	0.19019	75.12	0.0908	0.2496
Na^+(EC:DEC)	0.90411	0.0959	47.09	0.0747	0.1621

occurs from carbonate molecules to Na^+ ion. The amount of charge transfer (Δq_{Na^+}) between carbonate molecules and Na^+ ion in each complex is easily determined as the difference between the charge of isolated Na^+ ion and the charge of Na^+ ion in the corresponding complexes ($\Delta q_{Na^+} = q_{Na^+(isolated)} - q_{Na^+(complexed)}$).

The Natural Bond Orbital (NBO) analysis is also very useful for analyzing the binding mechanism of intermolecular interactions when the electron delocalization takes place. The energy decrease caused by the electron delocalization is generally estimated by the second-order perturbation energy (ΔE_{CT}). To investigate the donor−acceptor interactions in the formation of Na^+−O bonds in the studied complexes, a second-order perturbation theory analysis of the Fock matrix was carried out. The significant donor−acceptor orbital interactions in the formation of Na^+−O bonds occurs mostly between the lone pairs of oxygen atoms ($lp_{(O)}$) in carbonyl groups and the unoccupied orbital of lp* in Na^+ ion. The sum of ΔE_{CT} values for the formation of Na^+−O bonds in the studied complexes are listed in Table 2.

There is a fair correlation between binding energy (ΔE_b in kcal/mol) in the complexes of acyclic/cyclic carbonates and charge transfer values from acyclic/cyclic carbonates to Na^+ ion. As seen from Figure 5, ΔE_b values increase in these complexes when the charge transfer values increase.

In Bader's topological QTAIM analysis,[54] the nature of bonding is analyzed in terms of the properties of electron

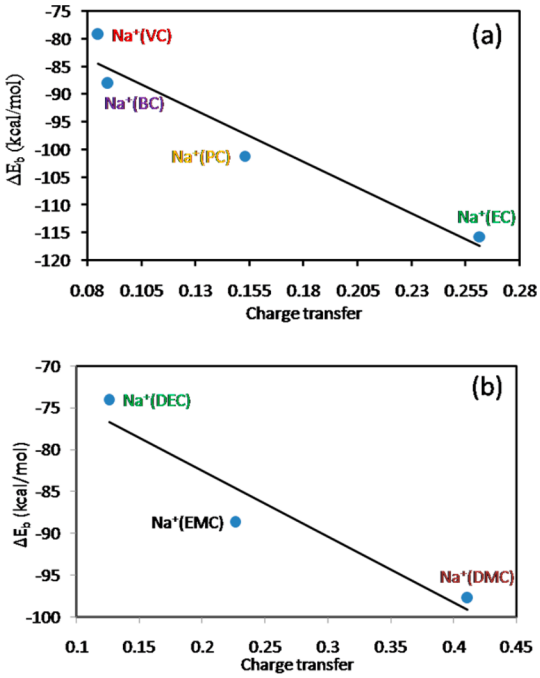

Figure 5. Correlation between binding energy (ΔE_b in kcal/mol) and charge transfer values for the complexes of cyclic carbonates (a) and acyclic carbonates (b) with Na^+ ion (r^2 = 0.928 and 0.910, respectively).

density and its derivatives. The Laplacian of electron density at the bond critical point (BCP), $\nabla^2\rho(r)$, which is defined as the sum of the three eigenvalues of the Hessian, λ_1, λ_2, and λ_3, is related to the bond interaction energy by local expression of the virial theorem[44]

$$\frac{1}{2}\nabla^2\rho(r) = 2G(r) + V(r) \tag{3}$$

where $G(r)$ is the electronic kinetic energy density, which is always positive, and $V(r)$ is the electronic potential energy density and must be always negative.[55] The sign of $\nabla^2\rho(r)$ at a BCP is determined by which energy is in excess over the viral average of 2:1 of kinetics to potential energy. In covalent interactions, the charge density at the BCP is tightly bound and compressed over its average distribution. Therefore, for covalent bonds, a negative value of $\nabla^2\rho(r)$ is expected, because $V(r)$ dominates in eq 3. On the other hand, in electrostatic interactions, the electronic charge is expanded relative to its average distribution. The kinetic energy density is dominant, and $\nabla^2\rho(r)$ is positive at the BCP. Apart from this, the electronic energy density, $H(r)$, as $H(r) = G(r) + V(r)$, evaluated at a BCP, can be used to compare the kinetic and potential energy densities on an equal footing. For all interactions with significant sharing of electrons, $H(r)$ is negative and its absolute value reflects covalent character of the interaction.[56] The QTAIM analysis was performed using AIM2000 program[57] at the M06-2X/6-311++G(d,p) level of theory.

The sum of electron density values ($\sum\rho(r)$) at the BCPs of Na^+−O bonds resulted from QTAIM analysis and the sum of Na^+−O Wiberg bond index ($\sum b_{Na^+-O}$) resulted from NPA analysis can be used for evaluation the bond strength of Na^+ ion with carbonate solvents. Figure 6 shows that there is a correlation between $\sum b_{Na^+-O}$ and $\sum\rho(r)$ in the Na-acyclic, Na-

DOI: 10.1021/acs.jpcc.5b04706
J. Phys. Chem. C 2015, 119, 22747−22759

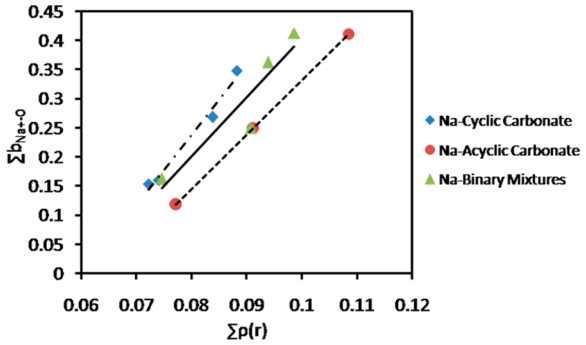

Figure 6. Correlation between the sum of Na^+−O Wiberg bond index ($\sum b_{Na^+-O}$) resulted from Natural Population Analysis (NPA) and the sum of electron density ($\sum \rho(r)$) at the bond critical points of Na^+−O bonds resulted from QTAIM analysis in the primary solvation sphere in the Na-acyclic, Na-cyclic, and Na-binary mixtures complexes (r^2 = 1, 0.980, 0.872, respectively).

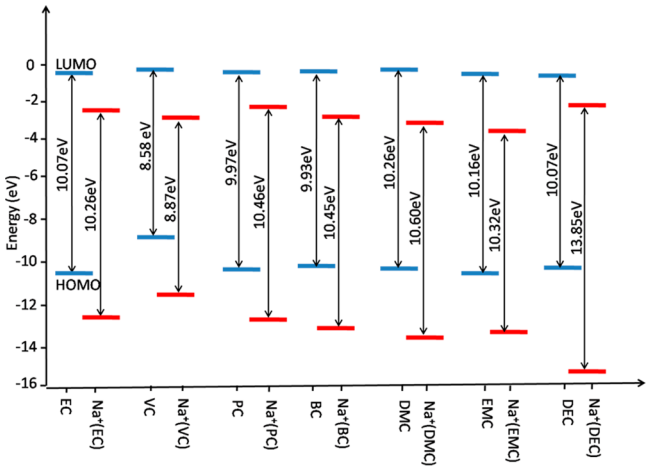

Figure 7. HOMO and LUMO energies of isolated carbonate solvents (EC, VC, PC, BC, DMC, EMC, and DEC) and their complexes.

cyclic, and Na-binary mixtures complexes. As seen from Figure 6, the highest sum of electron density ($\sum \rho(r)$) and sum of Na^+−O Wiberg bond index (b_{Na^+-O}) for the interaction of Na^+ ion with acyclic carbonates, cyclic carbonates, and binary mixtures are seen in the Na^+(EC), Na^+(DMC), and Na^+(EC:DMC) complexes, respectively.

The values of $\nabla^2\rho(r)$, $G(r)$, $V(r)$, and $H(r)$ for Na^+−O bonds in the complexes are calculated and summarized in Table S2 (see Supporting Information). It can be seen from Table S2 that all the values of $\nabla^2\rho(r)$ at the BCPs of Na^+−O bonds are positive. The positive sign of $\nabla^2\rho(r)$ indicates that these interactions should be classified as a closed-shell (electrostatic) type of bonding. On the other hand, all $H(r)$ values for the Na^+−O bonds are positive, suggesting a dominant electrostatic character.

3.4. Orbital Energy and Density of State (DOS) Calculations. We perform the density of state (DOS) calculation to investigate the variations in the electronic structure of a system as a result of changes in energetics due to molecular interactions.[58] An evaluation of the relative change in the band gap due to molecular interactions can also be obtained using DOS. DOS of a system describes the number of states per interval of energy at each energy level that are available to be occupied by electrons. A high value for the DOS at a particular energy interval suggests that multiple states are available for the occupation of the electrons, while a zero DOS indicates that no states are available for the electrons to be occupied at that particular energy interval. Further, the nonavailability of states for occupation by an electron at a particular energy interval represents the existence of a band gap.[58] Occupied states are known as the states with lower energies than the band gap, unoccupied states are known as the states with higher energies than the band gap. On the other hand, the highest occupied molecular orbital and the lowest unoccupied molecular orbital are named as HOMO and LUMO molecular orbitals, respectively. The energy difference between the HOMO and LUMO is termed the HOMO−LUMO (band) gap.

The HOMO, LUMO, and HOMO−LUMO energy gaps of carbonate molecules and their complexes with Na^+ ion are summarized in Table S3. As seen from Table S3, the HOMO−LUMO energy gap of carbonate molecules falls between 8.58 and 10.26 eV, and the band gap of their complexes changes from 8.87 to 13.85 eV. Figure 7 shows that the HOMO−LUMO energy gap in EC, VC, PC, BC, DMC, EMC, and DEC carbonate solvents increases as they interact with Na^+ ion. On the other hand, the HOMO−LUMO energy gap decreases with the addition of EC as an electrolyte additive to PC, DMC, EMC, and DEC carbonate solvents and their interaction with Na^+ ion (see Table S3).

To clarify the influence of ion complexing on the electronic structure of carbonate solvents, density of states (DOSs) for carbonate solvents, and their complexes are shown in Figure 8. As seen from Figure 8, the HOMO states in carbonate solvents are extended from −8.82 eV to the more negative energies, although the LUMO states are nearly extended from small negative values near zero to the positive energies. Upon interaction of the carbonate solvents with Na^+ ion, DOS featuring the carbonate solvents changes noticeably and energy shifts are observed. As seen from Table S3 and Figure 8, the HOMO and LUMO states of all carbonate solvents move to more negative energy values as they interact with Na^+ ion. For example, the HOMO and LUMO states of ethylene carbonate (EC) move to more negative energy values about 2.25 and 2.06 eV, respectively, as it interacts with Na^+ ion. These changes lead to an increase of 0.19 eV in the band gap of EC solvent.

3.5. Vibrational Frequency, Bond Length, and Electron Density of C═O Bonds. The interaction between the Na^+ ion and carbonate solvents can be further probed by analyzing their infrared (IR) spectra. Vibrational analysis on the optimized structures of acyclic and cyclic carbonates and their complexes with Na^+ ion shows that the most changes in vibrational frequencies are related to the carbonyl groups (C═O). The calculated infrared (IR) frequencies of C═O bonds in the carbonate solvents, and their complexes are listed in Table 3.

The C═O stretching frequencies in acyclic and cyclic carbonates and their mixtures can be affected by the presence of a Na^+ ion. It has been found that the stretching frequencies of C═O bonds become red-shifted after binding with Na^+ ion, indicating that C═O bonds are weakened. These changes in C═O vibrational frequencies are in line with the corresponding bond length and electron density changes. The C═O bond lengths increase with the metal complexing and the electron density values in the bond critical points of C═O bonds, resulted from QTAIM analysis, decrease. As seen from Figure 9, there is a correlation between the average of $\rho(r)$ in bond

DOI: 10.1021/acs.jpcc.5b04706
J. Phys. Chem. C 2015, 119, 22747−22759

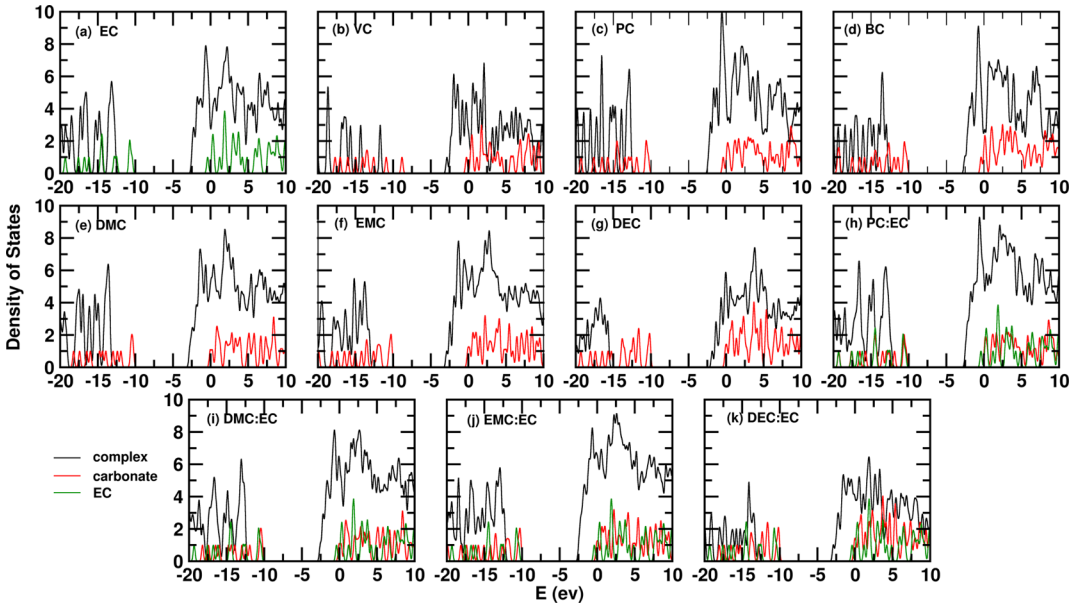

Figure 8. Density of states (DOSs) calculated at the M06-2X/6-311++G(d,p) level of theory before and after interaction of carbonate solvents with Na^+ ion.

Table 3. Vibrational Frequencies (ν in cm^{-1}), Bond Lengths (r in Å), and Electron Densities ($\rho(r)$ in e/au^3) of C═O Bonds in Isolated Carbonate Solvents and Their Complexes with Na^+ Ion

structure	$\nu_{(C=O)}$	$r_{(C=O)}$	$\rho(r)_{(C=O)}$	structure	$\nu_{(C=O)}$	$r_{(C=O)}$	$\rho(r)_{(C=O)}$
EC	1967.86	1.182	0.4387	Na^+(PC)	1938.67	1.196	0.4230
VC	1980.49	1.181	0.4398	Na^+(BC)	1911.91	1.201	0.4177
PC	1956.29	1.183	0.4381	Na^+(DMC)	1807.71	1.218	0.4044
BC	1961.62	1.183	0.4380	Na^+(EMC)	1802.87	1.219	0.4025
DMC	1854.70	1.201	0.4214	Na^+(DEC)	1790.55	1.222	0.3986
EMC	1851.82	1.202	0.4212	Na^+(EC:PC)	1934.89	1.198	0.4224
DEC	1846.97	1.202	0.4208	Na^+(EC:DMC)	1910.14	1.198	0.4232
Na^+(EC)	1918.20	1.201	0.4200	Na^+(EC:EMC)	1897.65	1.205	0.4156
Na^+(VC)	1930.70	1.199	0.4189	Na^+(EC:DEC)	1903.90	1.207	0.4120

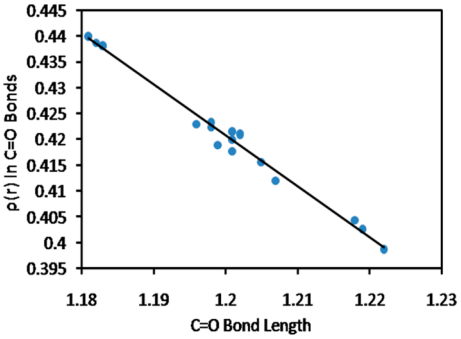

Figure 9. Correlation between the average of $\rho(r)$ in bond critical points of C═O bonds and the average of C═O bond lengths in Na-acyclic, Na-cyclic, and Na-binary mixture complexes (r^2 = 0.986).

critical points (BCPs) of C═O bonds and the average of C═O bond lengths in Na-acyclic, Na-cyclic, and Na-binary mixtures complexes. This correlation shows that the more C═O bond length, the less electron density values in BCPs of C═O bonds.

3.6. Localized Molecular Orbital Energy Decomposition Analysis (LMO-EDA). It is often desirable to obtain a reasonable and clear description of the component interaction energies contributing to the total noncovalent interaction energy when we need a deeper insight into the physical nature of this interaction.[59] The localized molecular orbital energy decomposition analysis (LMO-EDA), which was developed by Su et al.[45] and implemented in GAMESS software[46,47] calculations, was used to determine the contributions of interaction energy terms. In the LMO-EDA, the total interaction energy (ΔE_{int}) is decomposed into five terms:

$$\Delta E_{int} = \Delta E_{ele} + \Delta E_{ex} + \Delta E_{rep} + \Delta E_{pol} + \Delta E_{disp} \quad (4)$$

where ΔE_{ele} is the electrostatic energy, ΔE_{ex} is the exchange energy, ΔE_{rep} is the repulsion energy, ΔE_{pol} is the polarization energy, and ΔE_{disp} is the dispersion energy.[60] The LMO-EDA was carried out at the M06-2X/6-311++G(d,p) level of theory to determine the contributions of ΔE_{ele}, ΔE_{ex}, ΔE_{rep}, ΔE_{pol}, and ΔE_{disp} terms in the interaction energy between Na^+ ion and carbonate solvents.

Table 4 lists the LMO-EDA results for the Na^+-carbonate complexes. As seen from Table 4, the contribution of ΔE_{ele} component in each complex is more than other components. In addition, the contribution of ΔE_{ele}, ΔE_{ex}, ΔE_{pol}, and ΔE_{disp} terms in these complexes follows the order $\Delta E_{ele} > \Delta E_{pol} > \Delta E_{disp} > \Delta E_{ex}$. Based on the contribution of these components, it can be concluded that the nature of interaction in these complexes is electrostatic interaction. This result supports the results obtained from QTAIM analysis, which indicated that the

DOI: 10.1021/acs.jpcc.5b04706
J. Phys. Chem. C 2015, 119, 22747−22759

Table 4. LMO-EDA Results for the Na^+-Carbonate Complexes Calculated at the M06-2X/6-311++G(d,p) Level of Theory (All Energies are in kcal/mol)

structure	ΔE_{rep}	ΔE_{ex}	ΔE_{pol}	ΔE_{disp}	ΔE_{ele}	ΔE_{int}
Na^+(EC)	27.83	−5.13 (3.23%)	−30.71 (19.34%)	−12.53 (7.89%)	−110.41 (69.54%)	−130.96
Na^+(VC)	30.13	−6.67 (5.45%)	−26.02 (21.26%)	−8.2 (6.70%)	−81.52 (66.59%)	−92.28
Na^+(PC)	33.64	−7.07 (4.48%)	−31.41 (19.88%)	−10.54 (6.67%)	−108.95 (68.97%)	−124.33
Na^+(BC)	31.63	−7.06 (5.22%)	−27.26 (20.14%)	−8.52 (6.29%)	−92.52 (68.35%)	−103.74
Na^+(DMC)	46.51	−10 (6.95%)	−31.22 (21.69%)	−21.58 (14.99%)	−81.13 (56.37%)	−97.42
Na^+(EMC)	39.82	−8.65 (6.52%)	−29.29 (22.07%)	−15.89 (11.98%)	−78.87 (59.43%)	−92.88
Na^+(DEC)	36.52	−8.47 (7.25%)	−26.55 (22.74%)	−12.47 (10.69%)	−69.26 (59.32%)	−80.23
Na^+(EC:PC)	33.44	−6.58 (4.23%)	−32.05 (20.61%)	−15.04 (9.67%)	−101.84 (65.49%)	−122.07
Na^+(EC:DMC)	32.66	−6.21 (4.03%)	−29.93 (19.42%)	−17.01 (11.04%)	−100.94 (65.51%)	−121.43
Na^+(EC:EMC)	37.44	−8.08 (5.36%)	−30.90 (20.51%)	−13.92 (9.25%)	−97.74 (64.88%)	−113.21
Na^+(EC:DEC)	32.47	−7.27 (5.69%)	−26.67 (20.86%)	−8.89 (6.95%)	−85.05 (66.50%)	−95.41

interaction of Na^+ ion with carbonate solvents is electrostatic in nature.

3.7. Noncovalent Interactions (NCI) Analysis. For revealing the role and significance of noncovalent interactions in metal complexing of carbonate solvents, we used Multiwfn-3.2 program.[48] Noncovalent interactions (NCI) analysis enables the identification of noncovalent interactions and is based on the peaks that appear in the reduced density gradient (RDG) at low densities. When an RDG isosurface for a low value of RDG is plotted, the noncovalent regions clearly appear. These interactions correspond to both favorable and unfavorable interactions, as differentiated by the sign of the second density Hessian eigenvalue (λ_2). RDG isosurfaces are colored on a blue-green-red scale according to the strength and type (attractive or repulsive) of interaction. Blue indicates strong attractive interactions, green indicate weak van der Waals (vdW) interactions, and red indicates strong nonbonded overlap.

A qualitative noncovalent interaction (NCI) analysis has been performed to obtain more information about noncovalent interactions and more data about the behavior of the Na-acyclic, Na-cyclic, and Na-binary mixtures complexes. The visualization of noncovalent interactions between Na^+ ion and carbonate solvents in the real space was drawn using VMD 1.9.2 software[49] with an isosurface of 0.5 au and scale running from −0.020 (min) to 0.020 au (max). As seen from Figure 10, the blue−green region between Na^+ ion and carbonyl groups indicates that these interactions are strong to weak attractive interactions. On the other hand, the green regions between carbonate solvents also show that vdW interactions play a good role in putting carbonate solvents near together in Na-acyclic, Na-cyclic, and Na-binary mixtures complexes.

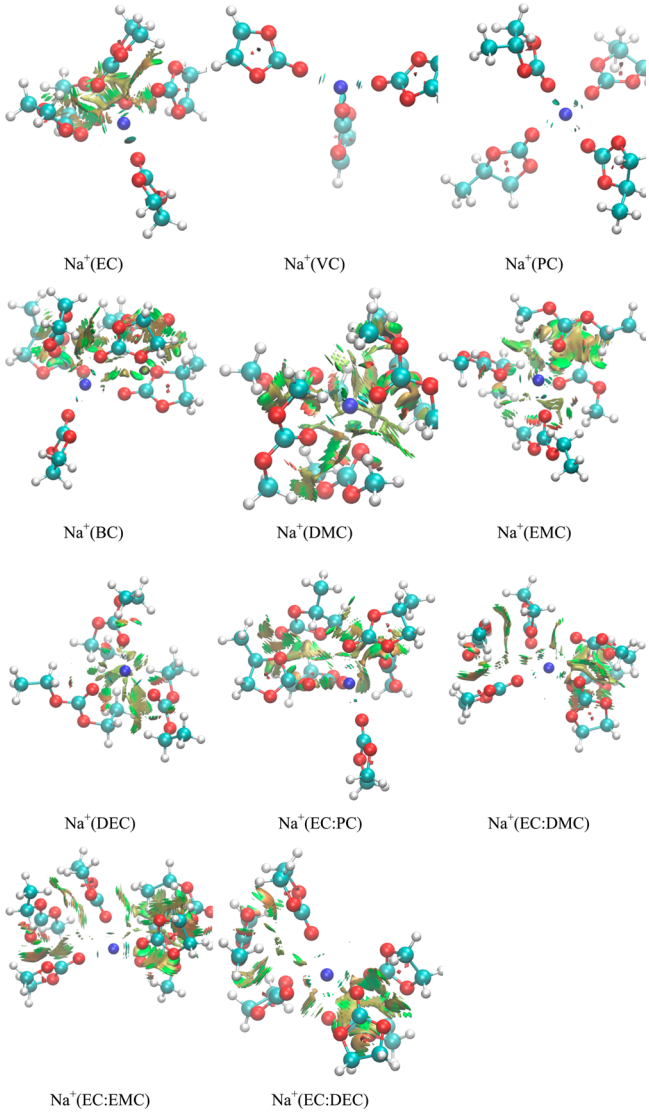

Figure 10. Three-dimensional view of reduced density gradient (RDG) calculation of Na-acyclic, Na-cyclic, and Na-binary mixtures complexes. Blue, green, and red colors indicate the strong attractive, weak vdW, and strong repulsion interactions, respectively.

4. CONCLUSIONS

To conclude, we evaluate the trends in the interaction of Na^+ ion with common nonaqueous electrolytes widely used as Na-ion battery electrolytes such as EC, VC, PC, BC, DMC, EMC, DEC, and EC-based binary mixtures (EC:PC, EC:DMC, EC:EMC, and EC:DEC) by using density functional theory at the M06-2X/6-311++G(d,p) level of theory. Our results suggest that the carbonate solvents interact with Na^+ ion via carbonyl oxygen in the primary solvation sphere. NBO analysis shows that the interactions occur mostly between the lone pairs of oxygen atom ($lp_{(O)}$) in carbonyl groups and the unoccupied orbital of lp* in Na^+ ion. The calculated infrared (IR) frequencies of C═O bonds in the carbonate solvents and their complexes show that the stretching frequency of C═O bonds become red-shifted after binding with Na^+ ion. These changes are in agreement with the bond length and electron density changes in C═O bonds.

DOI: 10.1021/acs.jpcc.5b04706
J. Phys. Chem. C 2015, 119, 22747−22759

The thermochemistry calculations show that the formation of Na^+ complexes is exothermic and proceeds favorably. The highest ΔE_b, $\Delta H_{(sol)}$, and $\Delta G_{(sol)}$ values for the interaction of Na^+ ion with EC, VC, PC, BC, DMC, EMC, and DEC carbonate solvents and the binary mixtures of EC:PC, EC:DMC, EC:EMC, and EC:DEC are seen for the Na^+(EC) and Na^+(EC:PC) complexes, respectively. On the other hand, the free energy of solvation of Na^+ ion in acyclic carbonates is less than cyclic carbonates and the $\Delta G_{(sol)}$ values decrease with the increase of the number of carbon atoms in acyclic and cyclic carbonates. Therefore, based on the $\Delta G_{(sol)}$ values in this study and the results of molecular dynamics simulations of these systems in our previous work, it could be concluded that EC and EC:PC electrolytes are better electrolytes than other alkyl carbonate based electrolytes for application in sodium ion batteries.

Density of state (DOS) calculations show that the HOMO and LUMO states of all carbonate solvents move to more negative energy values as they interact with Na^+ ion. The complexing of the ion with the electrolyte would make the electrolyte more prone to reduction by anode as the position of the bottom of the LUMO is shifted to lower energy. The increased band gap could widen the potential window on the other hand.

Our results also shows that the HOMO−LUMO energy gap in EC, VC, PC, BC, DMC, EMC, and DEC carbonate solvents increases upon interaction with Na^+ ion, although the HOMO−LUMO energy gap decreases with the addition of EC as an electrolyte additive to make binary solvents with PC, DMC, and EMC carbonate.

Our results indicate that binding energy (ΔE_b in kcal/mol) in Na-acyclic/cyclic complexes increases as the charge transfer values from acyclic/cyclic carbonates to Na^+ ion increase. On the other hand, the results of NBO analysis and QTAIM analysis show that there is a correlation between the sum of electron density values ($\sum\rho(r)$) at the BCPs of Na^+−O bonds and the sum of Na^+−O Wiberg bond index ($\sum b_{Na^+-O}$) in the Na-acyclic, Na-cyclic, and Na-binary mixtures complexes. Thus, $\sum\rho(r)$ and $\sum b_{Na^+-O}$ terms can be used for evaluation the bond strength of Na^+ ion with carbonate solvents.

QTAIM analysis shows that the interactions in Na-carbonate complexes are classified as a closed-shell (electrostatic) interaction. LMO-EDA also supports the nature of electrostatic interaction in Na-carbonate complexes and indicates that the contribution of ΔE_{ele}, ΔE_{ex}, ΔE_{pol}, and ΔE_{disp} terms in Na-carbonate complexes follows the order $\Delta E_{ele} > \Delta E_{pol} > \Delta E_{disp} > \Delta E_{ex}$. Overall, our electronic structure calculations provide fundamental insights into the trends in solvation behavior of Na^+ ion in the various commonly used battery electrolytes. The rank-order based on the various quantum calculations suggests EC:PC to be the best binary formulation, which is in excellent agreement with recent experiments.

■ ASSOCIATED CONTENT

Supporting Information

The Supporting Information is available free of charge on the ACS Publications website at DOI: 10.1021/acs.jpcc.5b04706.

The population distribution showing the percentage of various cluster sizes (Na-coordinated with various neat alkyl carbonates), the population analysis for various Na-coordinated carbonate clusters in the binary mixtures, the results of QTAIM analysis for Na^+−O bonds in the primary solvation sphere in Na-carbonate complexes, and the HOMO (in eV), LUMO (in eV), and HOMO−LUMO energy gaps (in eV) of the carbonate solvents and Na-carbonate complexes (PDF).

■ AUTHOR INFORMATION

Corresponding Authors

*E-mail: gkamath9173@gmail.com.

*E-mail: skrssank@anl.gov.

Notes

The authors declare no competing financial interest.

■ ACKNOWLEDGMENTS

Use of the Center for Nanoscale Materials was supported by the U.S. Department of Energy, Office of Science, Office of Basic Energy Sciences, under Contract No. DE-AC02-06CH11357.

■ REFERENCES

(1) Armand, M.; Tarascon, J. M. Building Better Batteries. *Nature* **2008**, *451*, 652−657.

(2) Dunn, B.; Kamath, H.; Tarascon, J. M. Electrical Energy Storage for the Grid: A Battery of Choices. *Science* **2011**, *334*, 928−935.

(3) Yang, Z.; Zhang, J.; Kintner-Meyer, M. C. W.; Lu, X.; Choi, D.; Lemmon, J. P.; Liu, J. Electrochemical Energy Storage for Green Grid. *Chem. Rev.* **2011**, *111*, 3577−3613.

(4) Thackeray, M. Lithium-Ion Batteries: An Unexpected Conductor. *Nat. Mater.* **2002**, *1*, 81−82.

(5) Xu, K. Nonaqueous Liquid Electrolytes for Lithium-Based Rechargeable Batteries. *Chem. Rev.* **2004**, *104*, 4303−4417.

(6) Tarascon, J. M.; Armand, M. Issues and Challenges Facing Rechargeable Lithium Batteries. *Nature* **2001**, *414*, 359−367.

(7) Kamath, G.; Cutler, R. W.; Deshmukh, S. A.; Shakourian-Fard, M.; Parrish, R.; Huether, J.; Butt, D. P.; Xiong, H.; Sankaranarayanan, S. K. R. S. In Silico Based Rank-Order Determination and Experiments on Nonaqueous Electrolytes for Sodium Ion Battery Applications. *J. Phys. Chem. C* **2014**, *118*, 13406−13416.

(8) Palomares, V.; Serras, P.; Villaluenga, I.; Hueso, K. B.; Carretero-Gonzalez, J.; Rojo, T. Na-Ion Batteries, Recent Advances and Present Challenges to Become Low Cost Energy Storage Systems. *Energy Environ. Sci.* **2012**, *5*, 5884−5901.

(9) Kim, S. W.; Seo, D. H.; Ma, X.; Ceder, G.; Kang, K. Electrode Materials for Rechargeable Sodium-Ion Batteries: Potential Alternatives to Current Lithium-Ion Batteries. *Adv. Energy Mater.* **2012**, *2*, 710−721.

(10) Liu, B.; Luo, T.; Mu, G.; Wang, X.; Chen, D.; Shen, G. Rechargeable Mg-Ion Batteries Based on WSe_2 Nanowire Cathodes. *ACS Nano* **2013**, *7*, 8051−8058.

(11) Yabuuchi, N.; Kubota, K.; Dahbi, M.; Komaba, S. Research Development on Sodium-Ion Batteries. *Chem. Rev.* **2014**, *114*, 11636−11682.

(12) Ponrouch, A.; Marchante, E.; Courty, M.; Tarascon, J. M.; Palacın, M. R. In Search of an Optimized Electrolyte for Na-Ion Batteries. *Energy Environ. Sci.* **2012**, *5*, 8572−8583.

(13) Coetzer, J. A New High Energy Density Battery System. *J. Power Sources* **1986**, *18*, 377−380.

(14) Park, Y. U.; Seo, D. H.; Kwon, H. S.; Kim, B.; Kim, J.; Kim, H.; Kim, I.; Yoo, H. I.; Kisuk, K. A New High-Energy Cathode for a Na-Ion Battery with Ultrahigh Stability. *J. Am. Chem. Soc.* **2013**, *135*, 13870−13878.

(15) Yildirim, H.; Greeley, J. P.; Sankaranarayanan, S. K. R. S. Concentration-Dependent Ordering of Lithiated Amorphous TiO_2. *J. Phys. Chem. C* **2013**, *117*, 3834−3845.

(16) Yildirim, H.; Greeley, J. P.; Sankaranarayanan, S. K. R. S. The Effect of Concentration on Li Diffusivity and Conductivity in Rutile TiO_2. *Phys. Chem. Chem. Phys.* **2012**, *14*, 4565−4576.

DOI: 10.1021/acs.jpcc.5b04706
J. Phys. Chem. C 2015, 119, 22747−22759

(17) Yildirim, H.; Greeley, J.; Sankaranarayanan, S. K. R. S. Effect of Concentration on the Energetics and Dynamics of Li Ion Transport in Anatase and Amorphous TiO_2. *J. Phys. Chem. C* **2011**, *115*, 15661−15673.
(18) Bhide, A.; Hofmann, J.; Dürr, A. K.; Janek, J.; Adelhelm, P. Electrochemical Stability of Non-Aqueous Electrolytes for Sodium-Ion Batteries and Their Compatibility with $Na(0.7)CoO_2$. *Phys. Chem. Chem. Phys.* **2014**, *16*, 1987−1998.
(19) Ponrouch, A.; Dedryvere, R.; Monti, D.; Demet, A. E.; Mba, J. M. A.; Croguennec, L.; Masquelier, C.; Johansson, P.; Palacin, M. R. Towards High Energy Density Sodium Ion Batteries Through Electrolyte Optimization. *Energy Environ. Sci.* **2013**, *6*, 2361−2369.
(20) Komaba, S.; Murata, W.; Ishikawa, T.; Yabuuchi, N.; Ozeki, T.; Nakayama, T.; Ogata, A.; Gotoh, K.; Fujiwara, K. Electrochemical Na Insertion and Solid Electrolyte Interphase for Hard-Carbon Electrodes and Application to Na-Ion Batteries. *Adv. Funct. Mater.* **2011**, *21*, 3859−3867.
(21) Bogle, X.; Vazquez, R.; Greenbaum, S.; Cresce, A. V. W.; Xu, K. Understanding Li^+-Solvent Interaction in Nonaqueous Carbonate Electrolytes with ^{17}O NMR. *J. Phys. Chem. Lett.* **2013**, *4*, 1664−1668.
(22) Ogara, J. F.; Nazri, G.; Macarthur, D. M. A Carbon-13 and Lithium-6 Nuclear-Magnetic Resonance Study of Lithium Perchlorate Poly (Ethylene-Oxide) Electrolytes. *Solid State Ionics* **1991**, *47*, 87−96.
(23) Fukushima, T.; Matsuda, Y.; Hashimoto, H.; Arakawa, R. Solvation of Lithium Ions in Organic Electrolytes of Primary Lithium Batteries by Electrospray Ionization-Mass Spectroscopy. *J. Power Sources* **2002**, *110*, 34−37.
(24) Bhatt, M. D.; Cho, M.; Cho, K. Interaction of Li^+ Ions with Ethylene Carbonate (EC): Density Functional Theory Calculations. *Appl. Surf. Sci.* **2010**, *257*, 1463−1468.
(25) Sekhon, S. S.; Deepa, M.; Agnihotry, S. A. Solvent Effect on Gel Electrolytes Containing Lithium Salts. *Solid State Ionics* **2000**, *136*−*137*, 1189−1192.
(26) Borodin, O.; Smith, G. D. Quantum Chemistry and Molecular Dynamics Simulation Study of Dimethyl Carbonate: Ethylene Carbonate Electrolytes Doped with $LiPF_6$. *J. Phys. Chem. B* **2009**, *113*, 1763−1776.
(27) Bhatt, M. D.; O'Dwyer, C. Density Functional Theory Calculations for Ethylene Carbonate-Based Binary Electrolyte Mixtures in Lithium Ion Batteries. *Curr. Appl. Phys.* **2014**, *14*, 349−354.
(28) Silva, L. B.; Freitas, L. C. G. Structural and Thermodynamic Properties of Liquid Ethylene Carbonate and Propylene Carbonate by Montecarlo Simulations. *J. Mol. Struct.: THEOCHEM* **2007**, *806*, 23−34.
(29) Borodin, O.; Smith, G. D. LiTFSI Structure and Transport in Ethylene Carbonate from Molecular Dynamics Simulations. *J. Phys. Chem. B* **2006**, *110*, 4971−4977.
(30) Okoshi, M.; Yamada, Y.; Yamada, A.; Nakai, H. Theoretical Analysis on De-Solvation of Lithium, Sodium, and Magnesium Cations to Organic Electrolyte Solvents. *J. Electrochem. Soc.* **2013**, *160*, 2160−2165.
(31) Sen, F. G.; Kinaci, A.; Narayanan, B.; Gray, S.; Davis, M. J.; Sankaranarayanan, S. K. R. S.; Chan, M. Towards Accurate Prediction of Catalytic Activity in IrO_2 Nanoclusters via First Principles-Based Variable Charge Force Field. *J. Mater. Chem. A* **2015**, *3*, 18970.
(32) Pukrittayakamee, A.; Malshe, M.; Hagan, M.; Raff, L. M.; Narulkar, R.; Bukkapatnum, S.; Komanduri, R. Simultaneous Fitting of a Potential-Energy Surface and Its Corresponding Force Fields Using Feedforward Neural Networks. *J. Chem. Phys.* **2009**, *130*, 134101−134110.
(33) Skarmoutsos, I.; Ponnuchamy, V.; Vetere, V.; Mossa, S. Li^+ Solvation in Pure, Binary and Ternary Mixtures of Organic Carbonate Electrolytes. *J. Phys. Chem. C* **2015**, *119*, 4502−4515.
(34) Soetens, J. C.; Millot, C.; Maigret, B. Molecular Dynamics Simulation of $Li^+BF_4^-$ in Ethylene Carbonate, Propylene Carbonate and Dimethyl Carbonate Solvents. *J. Phys. Chem. A* **1998**, *102*, 1055−1061.
(35) Postupna, O. O.; Kolesnik, Y. V.; Kalugin, O. N.; Prezhdo, O. V. Microscopic Structure and Dynamics of $LiBF_4$ Solutions in Cyclic and Linear Carbonates. *J. Phys. Chem. B* **2011**, *115*, 14563−14571.
(36) Tenney, C. M.; Cygan, R. T. Analysis of Molecular Clusters in Simulations of Lithium-Ion battery Electrolytes. *J. Phys. Chem. C* **2013**, *117*, 24673−24684.
(37) Phillips, J. C.; Braun, R.; Wang, W.; Gumbart, J.; Tajkhorshid, E.; Villa, E.; Chipot, C.; Skeel, R. D.; Kale, L.; Schulten, K. Scalable Molecular Dynamics with Namd. *J. Comput. Chem.* **2005**, *26*, 1781−1802.
(38) Vanommeslaeghe, K.; et al. Charmm General Force Field: A Force Field for Drug-Like Molecules Compatible with the Charmm All-Atom Additive Biological Force Fields. *J. Comput. Chem.* **2009**, *31*, 671−690.
(39) Frisch, M. J.; Trucks, G. W.; Schlegel, H. B.; Scuseria, G. E.; Robb, M. A.; Cheeseman, J. R.; Scalmani, G.; Barone, V.; Mennucci, B.; Petersson, G. A.; et al. *Gaussian 09*, Revision D.01; Gaussian, Inc.: Wallingford, CT, 2010.
(40) Zhao, Y.; Truhlar, D. G. The M06 Suite of Density Functionals for Main Group Thermochemistry, Thermochemical Kinetics, Noncovalent Interactions, Excited States, and Transition Elements: Two New Functionals and Systematic Testing of Four M06-Class Functionals and 12 Other Functionals. *Theor. Chem. Acc.* **2008**, *120*, 215−241.
(41) Boys, S. F.; Bernardi, F. The Calculation of Small Molecular Interactions by the Differences of Separate Total Energies. Some Procedures with Reduced Errors. *Mol. Phys.* **1970**, *19*, 553−566.
(42) Reed, A. E.; Curtiss, L. A.; Weinhold, F. Intermolecular Interactions from a Natural Bond Orbital, Donor-Acceptor Viewpoint. *Chem. Rev.* **1988**, *88*, 899−926.
(43) Reed, A. E.; Weinstock, R. B.; Weinhold, F. Natural Localized Molecular Orbitals. *J. Chem. Phys.* **1985**, *83*, 735−746.
(44) Bader, R. F. W. *Atom in Molecules: A Quantum Theory*; Oxford University Press: New York, 1990.
(45) Su, P.; Li, H. Energy Decomposition Analysis of Covalent Bonds and Intermolecular Interactions. *J. Chem. Phys.* **2009**, *131*, 014102−014116.
(46) Gordon, M. S.; Schmidt, W. W. Advances in Electronic Structure Theory: GAMESS a Decade Later. In *Theory and Applications of Computational Chemistry*; Dykstra, C. E., Frenking, G., Kim, K. S., Scuseria, G. E., Eds.; Elsevier: Amsterdam, The Netherlands, 2005; Chapter 41.
(47) Schmidt, M. W.; Baldridge, K. K.; Boatz, J. A.; Elbert, S. T.; Gordon, M. S.; Jensen, J. J.; Koseki, S.; Matsunaga, N.; Nguyen, K. A.; Su, S.; et al. *J. Comput. Chem.* **1993**, *14*, 1347−1363.
(48) Lu, T.; Chen, F. Multiwfn: A Multifunctional Wavefunction Analyzer. *J. Comput. Chem.* **2012**, *33*, 580−592.
(49) Humphrey, W.; Dalke, A.; Schulten, K. VMD: Visual Molecular Dynamics. *J. Mol. Graphics* **1996**, *14*, 33−38.
(50) Ahmadi, M. S.; Shakourian-Fard, M.; Fattahi, A. Molecular Structure and Character of Bonding of Mono and Divalent Metal Cations (Li^+, Na^+, K^+, Mg^{2+}, Ca^{2+}, Zn^{2+}, and Cu^+) with Guanosine: AIM and NBO Analysis. *Struct. Chem.* **2012**, *23*, 613−626.
(51) Shakourian-Fard, M.; Fattahi, A.; Jamshidi, Z. Interaction of Cations with 2′-Deoxythymidine Nucleoside and Analysis of the Nature and Strength of Cation Bonds. *J. Phys. Org. Chem.* **2012**, *25*, 153−161.
(52) Tjong, H.; Zhou, H. X. GBr^6: A Parameterization-Free, Accurate, Analytical Generalized Born Method. *J. Phys. Chem. B* **2007**, *111*, 3055−3061.
(53) Wiberg, K. Application of the Pople-Santry-Segal CNDO Method to the Cyclopropylcarbinyl and Cyclobutylcation and to Bicyclobutane. *Tetrahedron* **1968**, *24*, 1083−1096.
(54) Bader, R. W. F. A Quantum Theory of Molecular Structure and Its Applications. *Chem. Rev.* **1991**, *91*, 893−928.
(55) Bader, R. W. F. A Bond Path: A Universal Indicator of Bonded Interactions. *J. Phys. Chem. A* **1998**, *102*, 7314−7323.

DOI: 10.1021/acs.jpcc.5b04706
J. Phys. Chem. C 2015, 119, 22747−22759

(56) Jamshidi, Z.; Far, M. F.; Maghari, A. Binding of Noble Metal Clusters with Rare Gas Atoms: Theoretical Investigation. *J. Phys. Chem. A* **2012**, *116*, 12510−12517.
(57) Bader, R. F. W. *AIM2000 Program Package*, Version 2.0; McMaster University: Hamilton, Ontario, Canada, 2002.
(58) Ruuska, H.; Pakkanen, T. A. Ab Initio Study of Interlayer Interaction of Graphite: Benzene−Coronene and Coronene Dimer Two-Layer Models. *J. Phys. Chem. B* **2001**, *105*, 9541−9547.
(59) Szatylowicz, H.; Krygowski, T. M.; Solà, M.; Palusiak, M.; Dominikowska, J.; Stasyuk, O. A.; Poater, J. Why 1,2-Quinone Derivatives Are More Stable Than Their 2,3-Analogues? *Theor. Chem. Acc.* **2015**, *134*, 35−48.
(60) Niu, X.; Huang, Z.; Ma, L.; Shen, T.; Guo, L. Density Functional Theory, Natural Bond Orbital and Quantum Theory of Atoms in Molecule Analyses on the Hydrogen Bonding Interactions in Tryptophan-Water Complexes. *J. Chem. Sci.* **2013**, *125*, 949−958.

DOI: 10.1021/acs.jpcc.5b04706
J. Phys. Chem. C 2015, 119, 22747−22759